A MOLECULAR MODEL OF CYP2D6 CONSTRUCTED BY HOMOLOGY WITH THE CYP2C5 CRYSTALLOGRAPHIC TEMPLATE: INVESTIGATION OF ENZYME-SUBSTRATE INTERACTIONS

David F.V. Lewis[1,*], Maurice Dickins[2], Brian G. Lake[3] and Peter S. Goldfarb[1]

[1]*School of Biomedical and Molecular Sciences, University of Surrey, Guildford, Surrey,*
[2]*Pfizer Central Research, Ramsgate Road, Sandwich, Kent, and*
[3]*BIBRA International Limited, Carshalton, Surrey, UK*

SUMMARY

The results of homology modelling of CYP2D6 based on the mammalian P450 crystal structure of rabbit CYP2C5 are reported. It is found that many CYP2D6-selective substrates are able to fit closely within the putative active site of the enzyme where there are favourable contacts with complementary amino acid residues, including aspartate-301 which has been probed via site-directed mutagenesis. The homology model of CYP2D6 is consistent with available experimental evidence from selective substrate metabolism and site-specific mutation data. Quantitative structure-activity relationships (QSARs) with substrate binding affinity based on K_D values and inhibition data (K_i values) demonstrate the importance of hydrogen bonding, π-π stacking and relative molecular mass in describing variations in avidity towards the CYP2D6 enzyme, although the compound lipophilicity (log $D_{7.4}$) appears to be the most important single descriptor for CYP2D6 inhibition. Calculation of substrate

* Author for correspondence:
David F.V. Lewis
School of Biomedical and Molecular Sciences
University of Surrey
Guildford, Surrey, GU2 7XH, UK
e-mail: d.lewis@surrey.ac.uk

binding affinity based on contributions from active site interactions and lipophilic character gives satisfactory agreement with experimentally determined K_D values.

KEY WORDS

cytochrome P450, xenobiotic metabolism and activation, CYP2D6, homology modelling, CYP2C5 structural template

INTRODUCTION

The cytochromes P450 (CYP) constitute a superfamily of haemthiolate enzymes of which over 2,000 individual members are currently known, and these play key roles in both endogenous and exogenous metabolism of organic substrates in species from all five biological kingdoms /1-5/. In *Homo sapiens*, the majority of Phase 1 drug metabolism is catalyzed by P450 enzymes from families CYP1, CYP2 and CYP3 /6,7/, and about 40% of human P450-dependent drug metabolism is carried out by polymorphic enzymes /8/. The most important human drug-metabolizing P450 exhibiting polymorphism /9/ is CYP2D6, which mediates in about 20% of the known P450 oxidations for drugs in current clinical use /6/, and the activities of CYP2D6 allelic variants have also been reported /10/. Selective marker substrates for this enzyme include debrisoquine, bufuralol and metoprolol, whereas quinidine is a well-documented selective high-affinity inhibitor of CYP2D6 /11-14/. More recently, two high affinity substrates for the enzyme have been reported /15,16/ obtained, respectively, from investigation of a diltiazem metabolite and from novel compound design. Table 1 provides a summary of selected CYP2D6 substrates, their positions of metabolism and K_D values although, in some cases where K_D has not been measured, the K_S or K_m value is given instead.

In general, the characteristics of CYP2D6 substrates (Fig. 1, Table 1) include a basic nitrogen atom in the molecule, which is protonatable at physiological pH (pK_a values range from 8.3 to 13.01) and lying at a distance of either 5 or 7 Å from the site of metabolism, depending on the type of compound /17-25/. However, many (but not all) CYP2D6 substrates also contain an aromatic ring which either lies

TABLE 1

Physicochemical properties and metabolic pathways of selected CYP2D6 substrates

Compound	Metabolic pathway	log P	pK_a	log $D_{7.4}$	K_D (μM)	ΔG_{bind} (kcal.mol^{-1})
Bufuralol	1′-hydroxylation	3.50	9.0	1.89	8.6	-6.9535
Codeine	O-demethylation	1.07	8.2	0.23	15	-6.6218
Ondansetron	7-hydroxylation	2.14	7.7	1.30	102	-5.4790
Imipramine	2-hydroxylation	4.42	9.5	2.52	2.4	-7.7143
Desipramine	2-hydroxylation	4.05	10.0	1.45	20	-6.4503
Nortriptyline	10-hydroxylation	4.04	9.73	1.71	47	-5.9410
Amitriptyline	10-hydroxylation	5.04	9.4	2.50	74	-5.6703
Debrisoquine	4′-hydroxylation	0.75	13.01	0.75	13	-6.7071
Propranolol	4-hydroxylation	3.37	9.5	1.18	2.73	-7.6375
Dextromethorphan	O-demethylation	3.36	8.3	0.91	2.76	-7.6310
Metoprolol	O-demethylation	2.35	9.68	0.07	46 (K_S)	-6.4515
MDMA	O-demethylation	2.28	10.04	-0.27	1.72 (K_m)	-7.9129

K_D = enzyme-substrate dissociation constant; log P = logarithm of the octanol-water partition coefficient, P; pK_a = negative logarithm of the dissociation constant, K_a; log $D_{7.4}$ = logarithm of the distribution coefficient, D, at pH 7.4; M_r = relative molecular mass; MDMA = methylenedioxy-N-methylamphetamine; $\Delta G_{bind} = RT\ln K_D$ where K_D is the substrate dissociation constant (μM), R is the gas constant and T is the absolute temperature.
References: /30,39,40,48-50/.

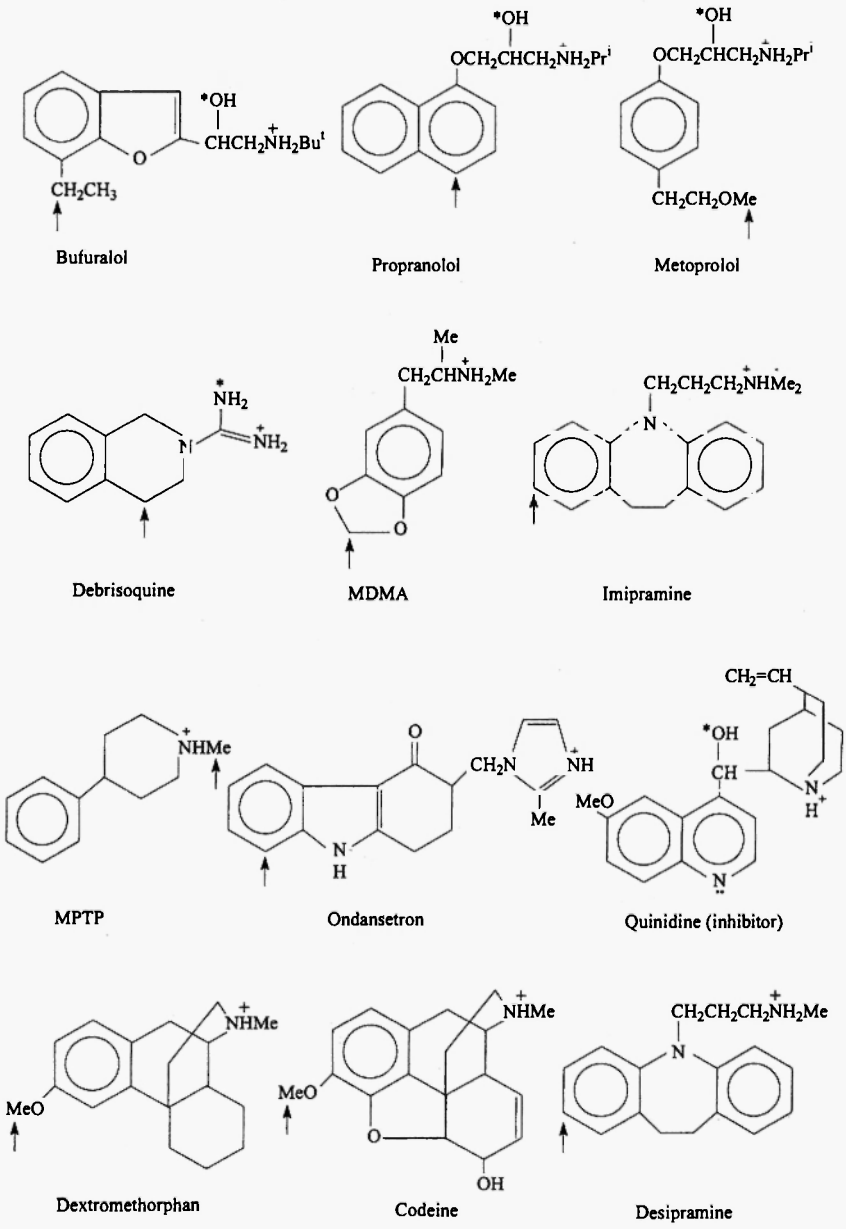

Fig. 1: A selection of typical CYP2D6 substrates showing their sites of metabolism (↑), position of positive charge (+) and location of hydrogen bond acceptors and donors (*).

close to the position of metabolism or includes it within the ring structure. Furthermore, there are hydrogen bond donor/acceptor atoms in the molecule, often at specific locations relative to the site of metabolism (see Fig. 1) but, again, this is not an essential feature of CYP2D6 substrates.

In order to investigate the potential utility of the recently available rabbit cytochrome P450 structure, CYP2C5 /26/, for homology modelling of human drug metabolizing P450s, we have constructed a three-dimensional model of CYP2D6 based on sequence alignment within the CYP2 family. We have also made use of information from substrate metabolism /27/ and site-directed mutagenesis studies /28-33,40-43/ to assist in the alignment process and also as a means of validating the model itself /27-46/.

METHODS

An alignment between a number of CYP2 family enzymes including CYP2D6 and that of the crystallographic template, CYP2C5, has been reported previously /36,42/. This multiple sequence alignment was generated using the GCG software package (Genetics Computer Group Inc., Madison, WI, USA) and involved a small amount of manual editing within the B-C loop region to account for an additional three residues (namely, ProArgSer) in CYP2D1 and CYP2D6 relative to the other CYP2 enzymes.

The raw model of CYP2D6 was constructed from the X-ray crystal structure coordinates /26/ of the CYP2C5 enzyme (pdb code: ldt6) using the Sybyl Biopolymer module (Tripos Associates Inc., St. Louis, MO, USA). This involved changing individual amino acid residues as required by the alignment with CYP2C5, together with a small number of short peptide insertions of no more than three residues in length. These were produced via loop searching of the protein databank using the Biopolymer module, and the most appropriate loop was chosen in each case on the grounds of homology and root mean square (rms) value relative to the peptide backbone surrounding the loop insertion. The raw model was initially refined to relax any unfavourable steric interactions produced by the first stages of the procedure, and this was then energy minimized via the Tripos force field to give a low energy geometry after several hundred iterative cycles of molecular mechanics.

The final enzyme model was then probed using known CYP2D6 substrates such that a molecular template of superimposed substrate molecules was produced within the putative active site. This involved interactive docking of each substrate on the basis of the proximity of its known site of metabolism to the haem iron and optimal ionic, hydrogen bond and π-π stacking interactions between the substrate and CYP2D6 active site amino acid residues. This process was facilitated by prior knowledge of site-directed mutagenesis studies (summarized in Table 2) on individual amino acid residues /28-33,40-43/, and by the inferred location of a docked substrate (progesterone) in CYP2C5 /26/.

All molecular modelling procedures were carried out using the Sybyl software package implemented on a Silicon Graphics Indigo^2 IMPACT 10000 graphics workstation operating under UNIX. K_D

TABLE 2

A summary of site-directed mutagenesis and allelic variants in SRS regions of CYP2D6

Change	2C5 †	SRS	Comments	References
T107I [a]	L103	1	lowers catalytic activity	/40/
E216G	L208	2	possible cationic contact	/33/
R296C [a]	V285	4	lowers catalytic activity	/41/
D301G	D290	4	main cationic contact	/28/
S304G	G293	4	possible hydrogen bond contact	/42,33/
V374M [a]	L363	5	affects metoprolol regioselectivity	/30/
L380F *	L363	5	affects bufuralol metabolism	/31/
F481L	N471	6	possible π-π stacking residue	/29/
F483I	F473	6	possible π-π stacking residue	/32/
S486T [a]	V476	6	lowers catalytic activity	/41/

a = allelic variant; * = site-specific mutagenesis in CYP2D1, the rat orthologue of CYP2D6; † = corresponding residue position in the CYP2C5 template.
Review reference: /43/.

values were determined by UV-visible spectroscopy using purified human P450 via methodology which has been described previously /27/. Briefly, this involved measurement of absorbance changes at 418 nm while keeping the enzyme concentration constant in 0.1 M phosphate buffer at pH 7.5, and varying substrate concentrations from 30 to 400 μM.

RESULTS AND DISCUSSION

Figure 2 shows the putative active site of CYP2D6 containing the bound substrate propranolol orientated for 4-hydroxylation via a combination of π-π stacking and electrostatic interactions with

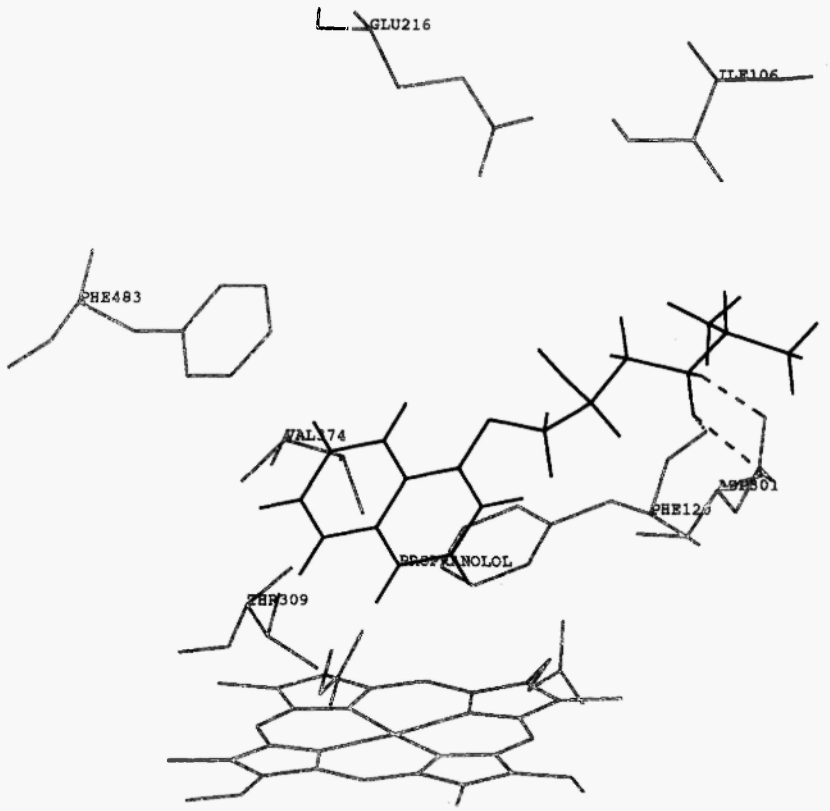

Fig. 2: The interaction between propranolol and the putative active site of CYP2D6. Hydrogen bonds are shown as dashed lines.

complementary amino acid residues. In particular, the side-chain of aspartate-301 forms an ion-pair with the protonated nitrogen atom of the substrate, and phenylalanine-483 enters into aromatic π-π stacking with the naphthalene ring of propranolol. There is also another π-π stacking interaction with the side-chain of phenylalanine-120, and the isopropyl group of propranolol forms hydrophobic contacts with leucine-121 and isoleucine-106 and possibly with another complementary residue, leucine-121, although this has been omitted from Figure 2 to improve clarity. These interactions cooperate in orientating the substrate such that the hydrogen atom in the 4-position of propranolol lies directly over the haem iron at a distance of 3.1 Å (Table 3). Of these residues contacting the substrate, aspartate-301 and phenylalanine-483 have been the subject of site-directed mutagenesis experiments in CYP2D6 /28,29/. Consequently, the active site interactions described above accord well with what is known from experimental findings reported on CYP2D6 and its substrates.

TABLE 3

Distances between sites of metabolism and haem iron for CYP2D6 substrates investigated in this study

Compound	Route of metabolism	Reference to metabolism data	Distance (Å)
Propranolol	4-hydroxylation	/27/	3.145
Debrisoquine	4′-hydroxylation	/28/	2.612
Bufuralol	1′-hydroxylation	/29/	4.017
Metoprolol	O-demethylation	/30/	3.102
MDMA	O-demethylation	/44/	3.986
MPTP	N-demethylation	/45/	3.713
Ondansetron	7-hydroxylation	/46/	3.430
Quinidine	inhibition	/32/	2.816 *

MDMA = methylenedioxy-N-methylamphetamine.
MPTP = 1-methyl-4-phenyl-1,2,3,6-tetrahydropyridine.
* Distance between quinoline nitrogen atom and haem iron.

Structurally related substrates, such as bufuralol and metoprolol, also fit well inside the CYP2D6 active site, making similar contacts with the nearby amino acid residues described above, such that a superimposed molecular template with these and propranolol can be produced, as shown in Figure 3. Another residue lying close to the active site orientations of metoprolol and bufuralol is valine-374, and this has also been investigated using site-specific mutation /30/. Substitution of valine at this point with methionine can be shown to have a marked effect on the regioselectivity of metoprolol metabolism,

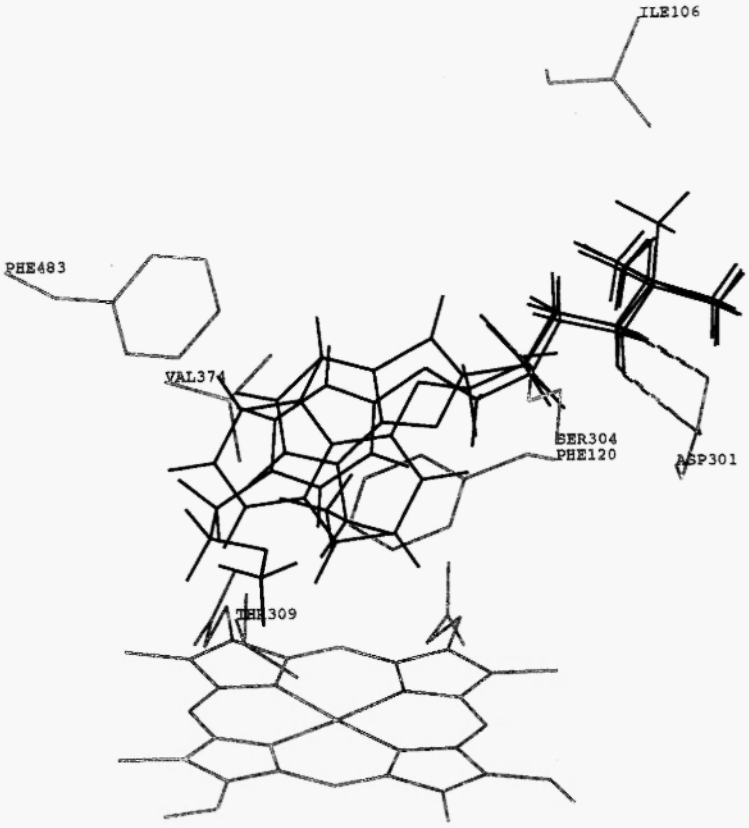

Fig. 3: A superimposed molecular template of selected CYP2D6 substrates (propranolol, bufuralol and metoprolol) based on proximity of site of metabolism to the haem iron and reinforced contacts with active site amino acid residues. Hydrogen bonds are displayed as dashed lines.

whereas alteration of the corresponding residue in the rat orthologue, CYP2D1, has been found to affect bufuralol metabolism /31/. The distance between the methoxy group (hydrogen) of metoprolol and the haem iron is 3.1 Å in the complex presented as Figure 3, whereas the 1′-position in bufuralol lies somewhat further from the iron atom at a distance of 4.0 Å in the CYP2D6 substrate template (Table 3).

Other amino acid residues present in the CYP2D6 active site region have also been investigated using site-directed mutagenesis. These include phenylalanine-481 /32/ and glutamate-216 /33,34/ both of which appear to have a role in the enzyme-substrate interaction (Table 2). It appears that glutamate-216 may be important /35/ in substrate recognition and access to the haem environment; this can be inferred from its position relative to the haem pocket, where it is located above the haem but possibly too far away from the active site to be directly involved in substrate binding associated with oxidation. In contrast, phenylalanine-481 has been proposed as a substrate contact residue /32/, although this appears to be somewhat removed from the main area of substrate binding within the haem locus of the CYP2D6 structure. As far as the current model is concerned, phenylalanine-483 seems more likely to act as one of the π-π stacking contacts with substrates containing aromatic rings at the appropriate position relative to the site of oxidation, but a role for phenylalanine-481 cannot be ruled out. In addition, valine-374 lies within the putative active site and acts as a hydrophobic contact for substrates in some cases, such as metoprolol (see Fig. 3). This residue has been shown to be responsible for the regioselectivity of metoprolol metabolism (O-demethylation) via a combination of techniques, including site-specific mutation /30/.

Consequently, the template of several typical CYP2D6 substrates overlaid within the active site exhibits a consistency with known experimental evidence. However, other substrates of the enzyme showing different structural characteristics also fit well within the current model. These include debrisoquine, MPTP, MDMA and ondansetron, where their respective sites of oxidation lie at distances of 2.6 Å, 3.7 Å, 3.9 Å and 3.5 Å from the haem iron, as listed in Table 3. In addition, Figure 4 provides a template of these substrates superimposed within the CYP2D6 active site where there are certain common contacts with nearby amino acid residues, including those mentioned previously. The model can, therefore, account for the fact

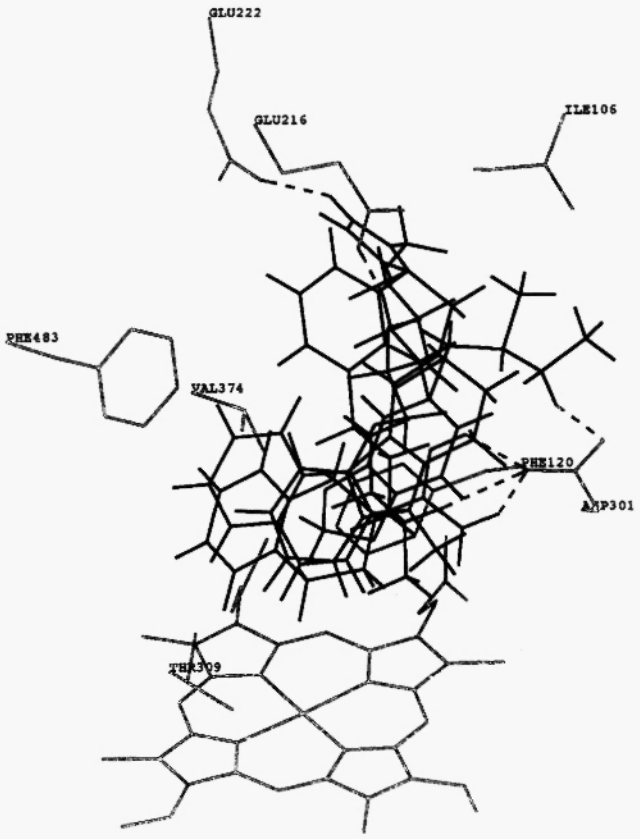

Fig. 4: A second template of CYP2D6 substrates including debrisoquine, MPTP, MDMA and ondansetron, orientated within the putative active site of CYP2D6. Hydrogen bonds are shown as dashed lines.

that unusual substrates such as MPTP are able to become metabolized via CYP2D6 at positions inconsistent with previously documented requirements for CYP2D6 selectivity, such as the possession of a protonated nitrogen at 4-7 Å from the site of metabolism. In the case of ondansetron, the imidazole nitrogen is weakly basic and lies at a distance greater than 7 Å from the known site of oxidation. Furthermore, the selective inhibitor, quinidine, can be shown to fit closely within the putative active site of CYP2D6 by entering into favourable contacts with complementary amino acid residues described previously,

including aspartate-301 which is common to all of the compounds mentioned in this study. The interaction shown in Figure 5 indicates that quinidine could interact with the haem iron via nitrogen ligation from the quinoline moiety, although this possibility remains to be verified experimentally.

QSARS AND ESTIMATION OF BINDING AFFINITY FOR CYP2D6 SUBSTRATES

Table 4A presents information relating to the properties of CYP2D6 substrates, and it is possible to make use of these data to

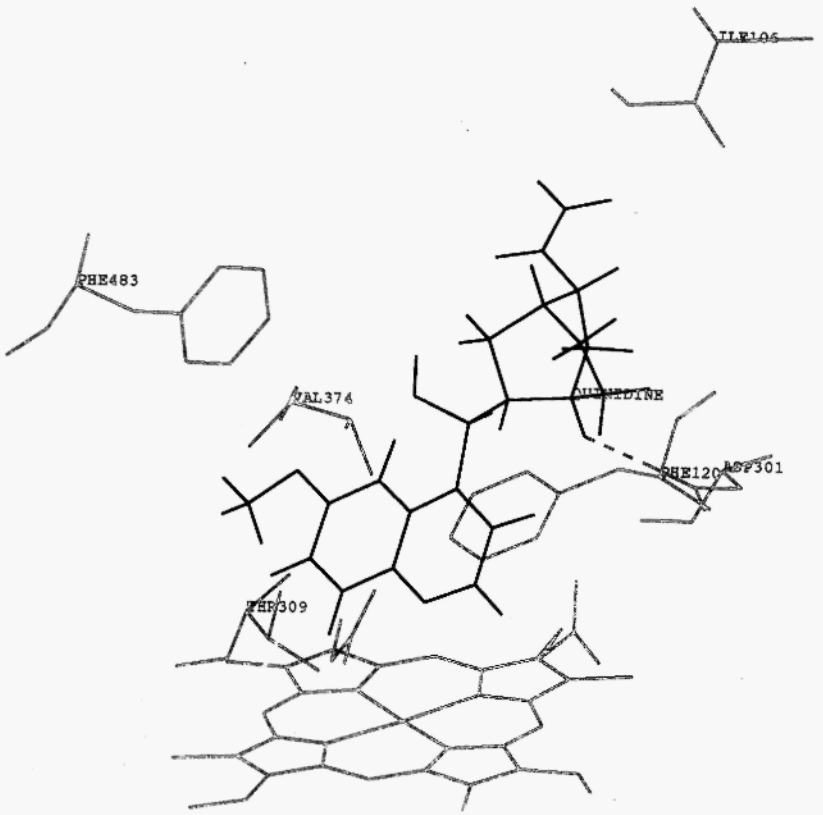

Fig. 5: The selective CYP2D6 inhibitor, quinidine, is shown orientated within the putative active site for haem ligation. Hydrogen bonds are displayed as dashed lines.

formulate quantitative relationships (QSARs) between structural characteristics and binding affinity towards CYP2D6, as determined by the enzyme-substrate K_D values. The energy of substrate binding, ΔG_{bind}, has been calculated from the K_D data using the expression $\Delta G_{bind} = RTlnK_D$, where R is the gas constant and T is the absolute temperature at which the K_D values were determined. In addition, information on inhibition of CYP2D6 has been collated from the literature /47/ and certain physico-chemical characteristics of the inhibitors are presented in Table 4B /48-50/. In this case, it appears that compound lipophilicity is important and the relative molecular mass does not exhibit a correlation with the K_i data. For substrates of CYP2D6, Table 4A provides the dataset which produced a QSAR for binding affinity towards CYP2D6. It can be appreciated that the numbers of hydrogen-bonded and π-π stacking interactions appear in the relevant QSAR expression (equation 1 in Table 4) which exhibits a fairly good agreement (R = 0.94) with experimental data. Additional descriptors relate to the overall size of the substrate molecule (relative molecular mass, M_r), and it is possible that this quantity may be associated with the desolvation of the active site on substrate binding. However, the appearance of the log M_r term may relate to the contribution made to the binding affinity due to loss in translational and rotational energy of the substrate upon binding to the enzyme /36/. It is unusual for both terms to be important in the QSAR; however, the correlation is significantly lowered when either is excluded. Nevertheless, one should exercise caution with regard to this expression due to the obvious similarity between the two descriptors associated with molecular size.

For CYP2D6 inhibitors, Table 4B shows the dataset which produced a very good correlation (R = 0.98) with inhibitory potency (pK_i values) and this relationship (equation 2 in Table 4) indicates that hydrogen bond potential and desolvation of the active site, together with overall substrate lipophilicity, help to explain the variation in inhibitory activity. The distribution coefficient (log $D_{7.4}$) also appears to show a linear relationship with pK_i values for a limited number of CYP2D6 inhibitors (seven out of a total of 11 compounds as shown in equation 3, Table 4) although one requires additional descriptors to explain the variation in activity for all 11 compounds, as exemplified by equation 2 in Table 4. Furthermore, a consideration of the various contributory factors to overall binding affinity (namely partitioning,

TABLE 4

QSARs for CYP2D6 substrate binding and inhibition /39,47/

A. CYP2D6 substrates

Compound	N_{HB}	$N_{\pi\pi}$	M_r	ΔG_{bind}
Bufuralol	3	1	261.36	-6.9535
Codeine	2	1	299.37	-6.6218
Ondansetron	2	1	293.40	-5.4790
Imipramine	2	2	280.41	-7.7143
Desipramine	2	2	266.39	-6.4503
Nortriptyline	2	2	263.38	-5.9410
Amitriptyline	2	2	263.38	-5.6703
Debrisoquine	1	1	175.23	-6.7071
Propranolol	3	1	259.35	-7.6375
Dextromethorphan	3	1	271.40	-7.6310

N_{HB} = number of hydrogen bonds; $N_{\pi\pi}$ = number of π-π stacking interactions; M_r = relative molecular mass; $\Delta G_{bind} = RT\ln K_D$ where K_D is the enzyme-substrate dissociation constant, R is the gas constant and T is the absolute temperature.

B. CYP2D6 inhibitors

Compound	N_B	H_A	M_r	log P	log $D_{7.4}$	pK_i
Oxprenolol	1	3	265.35	2.00	0.09	-1.0
Propranolol	1	2	259.35	3.37	1.18	-0.8261
Bufuralol	1	2	261.36	3.50	1.89	-0.6812
Citalopram	1	3	324.43	3.68	1.87	-0.7076
Amitriptyline	1	0	263.38	5.04	2.50	-0.6021
Chlorpromazine	1	1	318.86	5.40	2.79	-0.5798
Desmethylimipramine	1	1	266.39	4.05	1.45	-0.3617
Clomipramine	1	1	314.86	5.19	3.32	-0.3424
Levomepromazine	1	2	328.47	3.39	1.39	0.0
Yohimbine	1	3	354.49	2.59	2.18	0.3979
Quinidine	2	3	324.42	2.83	2.21	1.5229

N_B = number of basic nitrogens; H_A = number of hydrogen bond acceptors; log P = logarithm of the octanol/water partition coefficient; M_r = relative molecular mass; pK_i = log K_i where K_i is the inhibition constant; $D_{7.4}$ = distribution coefficient at pH 7.4.

Desmethylimipramine, levopromazine, yohimbine and quinidine were excluded from equation 3.

QSAR Expressions	n	s	R	F
1. ΔG_{bind} = 492.03 log M_r – 5.076 N_{HB} – 3.755 $N_{\pi\pi}$ – 0.880 M_r – 947.68 (±100.04) (±0.900) (±0.817) (±0.181)	10	0.3727	0.941	9.61
2. pK_i = 1.75 N_B – 0.57 H_A + 0.014 M_r – 0.48 log P – 3.56 (±0.21) (±0.15) (±0.002) (±0.13)	11	0.1874	0.979	35.17
3. pK_i = 0.187 log $D_{7.4}$ – 1.041 (±0.020)	7	0.0478	0.93	95.09

hydrogen bonding, π-π stacking and rotational energy) can lead to a satisfactory agreement (R = 0.98) with experimental ΔG_{bind} values of CYP2D6 substrates, as shown in Table 5. In this case, eight out of the ten compounds investigated gave an excellent agreement (R^2 = 0.96) with experiment, whereas desipramine appears to be a slight outlier, possibly due to an over-estimation of the lipophilic contribution to the binding affinity. Nevertheless, the agreement between experimental and calculated binding energies is good (R^2 = 0.95) for the inclusion of desipramine; and for all ten compounds the correlation is still satisfactory for the substrates under consideration.

This type of approach is also applicable to other human P450s involved in Phase 1 drug metabolism /36,37/. Compound lipophilicity has also been shown to have importance in CYP2D6 substrate binding /38/, albeit for a relatively small number of compounds. However, when the effect of substrate ionisation is taken into account (i.e. by consideration of the log $D_{7.4}$ value) there appears to be a good correlation (R = 0.98) with CYP2D6 inhibition as shown in Table 4. Nevertheless, it is necessary to include a different set of descriptors (although related to log $D_{7.4}$) in order to give a satisfactory explanation of the full set of inhibition data presented, and equation 2 in Table 4 provides this information. In this case, log P is involved in the QSAR expression, together with the number of basic nitrogens, number of hydrogen bond acceptors and relative molecular mass of the substrate, thus showing that a combination of factors explains the inhibition data for 11 compounds (R = 0.98). Clearly, therefore, lipophilicity is important for substrate and inhibitor interaction with CYP2D6, although other factors such as hydrogen bond potential and number of π-π stacking interactions need to be included to explain the variation in biological data relating to CYP2D6 activity. It would not be appropriate to combine the datasets for substrates and inhibitors, however, due to the fact that the biological quantities, namely K_D and K_i, respectively, are quite different parameters and measured via entirely different procedures. However, when examined separately, the data for substrates and inhibitors of CYP2D6 exhibit both similarities and differences in terms of the various compound descriptors which correlate with activity in each case.

TABLE 5

Comparison between experimental and calculated binding affinity

Compound	log P	ΔG_{part}	ΔG_{ionic}	ΔG_{hb}	$\Delta G_{\pi-\pi}$	ΔG_{rot}	ΔG^{calc}_{bind}	ΔG^{expt}_{bind}
Bufuralol	3.50	-4.9646	-4.0	-2.0	-0.9	4.8	-7.0646	-6.9535
Codeine	1.07	-1.5178	-4.0	0	-0.9	0	-6.4178	-6.6218
Ondansetron	2.14	-3.0355	0	-2.0	-0.9	0.6	-5.3355	-5.4790
Imipramine	4.42	-6.2696	-4.0	0	-0.9	3.6	-7.5696	-7.7143
Desipramine	4.05	-5.7448	-4.0	0	-0.9	3.6	-7.0448	-6.4508
Nortriptyline	4.04	-5.7306	-4.0	0	0	3.6	-6.1306	-5.9410
Amitriptyline	5.04	-7.1491	-4.0	0	0	3.6	-7.5491	-5.6703
Debrisoquine	0.75	-1.0638	-4.0	-2.0	-0.9	1.2	-6.7638	-6.7071
Propranolol	3.37	-4.7802	-4.0	-2.0	-0.9	4.2	-7.4802	-7.6375
Dextromethorphan	3.36	-4.7660	-4.0	0	0	0.6	-8.1660	-7.9129

$\Delta G_{part} = -RT\ln P$ where P is the octanol-water partition coefficient; ΔG_{ionic} = ionic interaction energy (-4.0 kcal.mol^{-1} per ionic interaction); ΔG_{hb} = hydrogen bond energy (-2.0 kcal mol^{-1} per hydrogen bond interaction); $\Delta G_{\pi-\pi}$ = π-π stacking energy (0.9 kcal.mol^{-1} per π-π stacking interaction); ΔG_{rot} = rotatable bond energy (0.6 kcal.mol^{-1} per rotatable bond restricted on binding).

$\Delta G^{calc}_{bind} = \Delta G_{part} + \Delta G_{ionic} + \Delta G_{hb} + \Delta G_{\pi-\pi} + \Delta G_{rot}$; ΔG^{expt}_{bind} = experimental binding energy given by $RT\ln K_D$ where K_D is the enzyme-substrate dissociation constant (μM), R is the gas constant and T is the absolute temperature.

The correlations between calculated and experimental binding affinities are $R^2 = 0.96$ for eight compounds (excluding desipramine and amitriptyline) and $R^2 = 0.95$ for nine compounds (excluding amitriptyline).

CONCLUSIONS

The generation of a 3D model of CYP2D6 from the CYP2C5 crystal structure provides a means of explaining several features of CYP2D6 substrate selectivity and metabolism. In general, the model is consistent with experimental evidence from site-directed mutagenesis and the known CYP2D6-mediated metabolism of typical substrates. Moreover, QSAR analyses of substrates and inhibitors of CYP2D6 can lead to an understanding of the likely factors involved in binding to the enzyme, and this is underscored by a satisfactory agreement between experimental binding affinity and that derived from a consideration of the potential contributions to overall binding energy in selected CYP2D6 substrates. It is hoped that this type of approach may also be applicable to other examples of P450-substrate interactions.

ACKNOWLEDGEMENTS

The financial support of GlaxoSmithKline Research and Development Limited, Merck Sharp & Dohme Limited and the University of Surrey Foundation Fund is gratefully acknowledged by DFVL. The help of Dr. Sandeep Modi (GSK) is also gratefully acknowledged for the generation of substrate K_D values.

REFERENCES

1. Anzenbacher P, Anzenbacherova E. Cytochromes P450 and metabolism of xenobiotics. Cell Mol Life Sci 2001; 58: 737-747.
2. Nelson, DR. Metazoan cytochrome P450 evolution. Comp Biochem Physiol C 1998; 121: 15-22.
3. Nelson DR. Cytochrome P450 and the individuality of species. Arch Biochem Biophys 1999; 369: 1-10.
4. Lewis DFV. Cytochrome P450: Structure, Function and Mechanism. London: Taylor & Francis, 1996.
5. Lewis DFV. Guide to Cytochromes P450 Structure and Function. London: Taylor & Francis, 2001.
6. Rendic S, DiCarlo FJ. Human cytochrome P450 enzymes: a status report summarizing their reactions, substrates, inducers and inhibitors. Drug Metab Rev 1997; 29: 413-580.
7. Evans WE, Relling MV. Pharmacogenetics: translating functional genomics into rational therapeutics. Science 1999; 286: 487-491.

8. Ingelman-Sundberg M, Oscarson M, McLellan RA. Polymorphic human cytochrome P450 enzymes: an opportunity for individualized drug treatment. Trends Pharmacol Sci 1999; 20: 342-349.
9. Marez D, Legrand M, Sabbagh N, Lo Guidice J-M, Spire C, Laffitte J-J, Meyer UA, Broly F. Polymorphism of the cytochrome P450 CYP2D6 gene in a European population: characterization of 48 mutations and 53 alleles, their frequencies and evolution. Pharmacogenetics 1997; 7: 193-202.
10. Marcucci KA, Pearce RE, Crespi C, Steimel DT, Leeder JS, Gaedigk A. Characterization of cytochrome P4502D6.1 (CYP2D6.1), CYP2D6.2 and CYP2D6.17 activities toward model CYP2D6 substrates dextromethorphan, bufuralol and debrisoquine. Drug Metab Dispos 2002; 30: 595-601.
11. Lennard MS, Tucker GT, Silas JH, Woods HF. Debrisoquine polymorphism and the metabolism and action of metoprolol, timolol, propranolol and atenolol. Xenobiotica 1986; 16: 435-447.
12. Gonzalez FJ. The CYP2D subfamily. In: Ioannides C, ed. Cytochromes P450 Metabolic and Toxicological Aspects, Ch. 8. Boca Raton, FL: CRC Press, 1996; 183-210.
13. Otton SV, Crewe HK, Lennard MS, Tucker GT, Woods HF. Use of quinidine inhibition to define the role of the sparteine/debrisoquine cytochrome P450 in metoprolol oxidation by human liver microsomes. J Pharmacol Exp Ther 1988; 247: 242-247.
14. Wolff T, Dislerath LM, Worthington MT, Groopman JD, Hammons GJ, Kadlubar FF, Prough RA, Martin MV, Guengerich FP. Substrate specificity of human liver cytochrome P450 debrisoquine 4-hydroxylase probed using immunochemical inhibition and chemical modeling. Cancer Res 1985; 45: 2116-2122.
15. Molden E, Asberg A, Christensen H. Desacetyl-diltiazem displays several fold higher affinity to CYP2D6 compared with CYP3A4. Drug Metab Dispos 2002; 30: 1-3.
16. Onderwater RCA, Venhorst J, Commandeur JNM, Vermeulen NPE. Design, synthesis and characterization of 7-methoxy-4-(aminomethyl)-coumarin as a novel and selective cytochrome P450 2D6 substrate suitable for high-throughput screening. Chem Res Toxicol 1999; 12: 555-559.
17. Ekins S, de Groot MJ, Jones JP. Pharmacophore and three-dimensional quantitative structure activity relationship methods for modeling cytochrome P450 active sites. Drug Metab Dispos 2001; 29: 936-944.
18. de Groot MJ, Ackland MJ, Horne VA, Alex AA, Jones BC. Novel approach to predicting P450-mediated drug metabolism: development of a combined protein and pharmacophore model for CYP2D6. J Med Chem 1999; 42: 1515-1524.
19. de Groot MJ, Bijloo GJ, van Acker FAA, Fonseca Guerra C, Snijders JG, Vermeulen NPE. Extension of a predictive substrate model for human cytochrome P450 2D6. Xenobiotica 1997; 27: 357-368.
20. de Groot MJ, Vermeulen NPE, Kramer JD, van Acker FAA, Donné-Op den Kelder GM. A three-dimensional protein model for human cytochrome P450

2D6 based on the crystal structures of P450 101, P450 102 and P450 108. Chem Res Toxicol 1996; 9: 1079-1091.
21. Lewis DFV, Eddershaw PJ, Goldfarb PS, Tarbit MH. Molecular modelling of cytochrome P4502D6 (CYP2D6) based on an alignment with CYP102: structural studies on specific CYP2D6 substrate metabolism. Xenobiotica 1997; 27: 319-340.
22. Islam SA, Wolf CR, Lennard MS, Sternberg MJE. A three-dimensional molecular template for substrates of human cytochrome P450 involved in debrisoquine 4-hydroxylation. Carcinogenesis 1991; 12: 2211-2219.
23. Koymans L, Vermeulen NPE, van Acker SABE, te Koppele JM, Heykants JJP, Lavrijsen K, Meuldermans W, Donné-Op den Kelder GM. A predictive model for substrates of cytochrome P450-debrisoquine (IID6). Chem Res Toxicol 1992; 5: 211-219.
24. Koymans LMH, Vermeulen NPE, Baarslag A, Donne-Op den Kelder GM. A preliminary 3D model for cytochrome P450 2D6 constructed by homology model building. J Comp-Aided Mol Design 1993; 7: 281-289.
25. Modi S, Paine MJ, Sutcliffe MJ, Lian L-Y, Primrose WU, Wolf CR, Roberts GCK. A model for human cytochrome P450 2D6 based on homology modeling and NMR studies of substrate binding. Biochemistry 1996; 35: 4540-4550.
26. Williams PA, Cosme J, Sridhar V, Johnson EF, McRee DE. Mammalian cytochrome P450 monooxygenase: structural adaptations for membrane binding and functional diversity. Mol Cell 2000; 5: 121-131.
27. Lewis DFV, Modi S, Dickins M. Quantitative structure-activity relationships (QSARs) within substrates of human cytochromes P450 involved in drug metabolism. Drug Metab Drug Interact 2001; 18: 221-242.
28. Ellis SW, Hayhurst GP, Smith G, Lightfoot T, Wong MMS, Simula AP, Ackland MJ, Sternberg MJE, Lennard MS, Tucker GT, Wolf GR. Evidence that aspartic acid 301 is a critical substrate-contact residue in the active site of cytochrome P450 2D6. J Biol Chem1995; 270: 29055-29058.
29. Smith G, Modi S, Pillai I, Lain L-Y, Sutcliffe MJ, Pritchard MP, Friedberg T, Roberts GCK, Wolf CR. Determinants of the substrate specificity of human cytochrome P450 CYP2D6: design and construction of a mutant with testosterone hydroxylase activity. Biochem J 1998; 331: 783-792.
30. Ellis SW, Rowland K, Ackland MJ, Rekka E, Simula AP, Lennard MS, Wolf CR, Tucker GT. Influence of amino acid residue 374 of cytochrome P450 2D6 (CYP2D6) on the regio- and enantio-selective metabolism of metoprolol. Biochem J 1996; 316: 647-654.
31. Matsunaga E, Zeugin T, Zanger UM, Aoyama T, Meyer UA, Gonzalez FJ. Sequence requirements for cytochrome P450IID1 catalytic activity. J Biol Chem 1990; 265: 17197-17201.
32. Hayhurst GP, Harlow J, Chowdry J, Gross E, Hilton E, Lennard MS, Tucker GT, Ellis SW. Influence of phenylalanine-481 substitutions on the catalytic activity of cytochrome P450 2D6. Biochem J 2001; 355: 373-379.
33. Ellis SW. Active site residues of CYP2D6 - fact or fiction? Proc Australian Soc Clin Exp Pharmacol Toxicol 2000; 7: 12.

34. Ellis SW, Harlow J, Chowdry J, Tucker GT. Active-site residues of CYP2D6 - fact and fiction. 12th International Conference on Cytochrome P450, La Grande Motte, France, September 11-15, 2001; 70.
35. Venhorst J, Onderwater RCA, Meerman JHN, Commandeur JNM, Vermeulen NPE. Influence of N-substitution on 7-methoxy-4-(aminomethyl)-coumarin on cytochrome P450 metabolism and selectivity. Drug Metab Dispos 2000; 28: 1524-1532.
36. Lewis DFV. On the recognition of mammalian microsomal cytochrome P450 substrates and their characteristics. Biochem Pharmacol 2000; 60: 293-306.
37. Lewis DFV. Homology modelling of human CYP2 family enzymes based on the CYP2C5 crystal structure. Xenobiotica 2002; 32: 305-323.
38. Ferrari S, Leemann T, Dayer P. The role of lipophilicity in the inhibition of polymorphic cytochrome P450IID6 oxidation by beta-blocking agents in vitro. Life Sci 1991; 48: 2259-2265.
39. Lewis DFV, Modi S, Dickins M. Structure-activity relationships for human cytochrome P450 substrates and inhibitors. Drug Metab Rev 2002; 34: 69-82.
40. Tucker GT, Lennard MS, Ellis SW, Woods HF, Cho AK, Lin LY, Hiratsuka A, Schmitz DA, Chu TYY. The demethylenation of methylenedioxymethamphetamine ("ecstasy") by debrisoquine hydroxylase (CYP2D6). Biochem Pharmacol 1994; 47: 1151-1156.
41. Daly AK, Brockmöller J, Broly F, Eichelbaum M, Evans WE, Gonzalez FJ, Huang J-D, Idle JR, Ingelman-Sunderg M, Ishizaki T, Jacqz-Aigrain E, Meyer UA, Nebert DW, Steen VM, Wolf CR, Zanger UM. Nomenclature for human CYP2D6 alleles. Pharmacogenetics 1996; 6: 193-201.
42. Mackman R, Tschirret-Guth RA, Smith G, Hayhurst GP, Ellis SW, Lennard MS, Tucker GT, Wolf CR, Ortiz de Montellano PR. Active-site topology of human CYP2D6 and its aspartate-301→glutamate, asparagine and glycine mutants. Arch Biochem Biophys 1996; 331: 134-140.
43. Lewis DFV. The CYP2 family: models, mutants and interactions. Xenobiotica 1998; 28: 617-661.
44. Tucker GT, Lennard MS, Ellis SW, Woods HF, Lin L, Hiratsuka A, Chu T, Cho AK. 'Ecstasy' is demethylenated by human cytochrome P450 2D6 (CYP2D6). Br J Clin Pharmacol 1993; 36: 144P.
45. Modi S, Gilham DE, Sutcliffe MJ, Lian L-Y, Primrose WU, Wolf CR, Roberts GCK. 1-Methyl-4-phenyl-1,2,3,6-tetrahydropyridine as a substrate of cytochrome P4502D6: allosteric effects of NADPH-cytochrome P450 reductase. Biochemistry 1997; 36: 4461-4470.
46. Fischer V, Vickers AEM, Heitz F, Mahadevan S, Baldeck J-P, Minery P, Tynes R. The polymorphic cytochrome P450 2D6 is involved in the metabolism of both 5-hydroxytryptamine antagonists, tropisetron and ondansetron. Drug Metab Dispos 1994; 22: 269-274.
47. Smith DA, Jones BC. Speculations on the substrate structure-activity relationship (SSAR) of cytochrome P450 enzymes. Biochem Pharmacol 1992; 44: 2089-2098.
48. Hansch C, Leo A, Hoekman D. Exploring QSAR: Hydrophobic, Electronic and Steric Constants. Washington, DC: American Chemical Society, 1995.

49. Dollery C. Therapeutic Drugs. Edinburgh: Churchill-Livingstone, 1999.
50. Newton DW, Kluza RB. pK_a values of medicinal compounds in pharmacy practice. Drug Intelligence Clin Pharm 1978; 12: 546-554.